Talanta 119 (2014) 447–451

Contents lists available at ScienceDirect

Talanta

journal homepage: www.elsevier.com/locate/talanta

Polypyrrole/multi-walled carbon nanotube composite for the solid phase extraction of lead(II) in water samples

Ertugrul Sahmetlioglu [a], Erkan Yilmaz [b], Ece Aktas [a], Mustafa Soylak [b,*]

[a] Nigde University, Faculty of Sciences and Arts, Chemistry Department, 51100 Nigde, Turkey
[b] Erciyes University, Faculty of Sciences, Chemistry Department, 38039 Kayseri, Turkey

ARTICLE INFO

Article history:
Received 14 August 2013
Received in revised form
10 November 2013
Accepted 15 November 2013
Available online 27 November 2013

Keywords:
Conducting polymer
Multi-walled carbon nanotubes
Nanocomposite
Lead
Solid phase extraction

ABSTRACT

A multi-walled carbon nanotubes-polypyrrole conducting polymer nanocomposite has been synthesized, characterized and used for the separation and preconcentration of lead at trace levels in water samples prior to its flame atomic absorption spectrometric detection. The analytical parameters like pH, sample volume, eluent, sample flow rate that were affected the retentions of lead(II) on the new nanocomposite were optimized. Matrix effects were also investigated. Limit of detection and preconcentration factors were 1.1 μg L^{-1} and 200, respectively. The adsorption capacity of the nanocomposite was 25.0 mg lead(II) per gram composite. The validation of the method was checked by using SPS-WW2 Waste water Level 2 certified reference material. The method was applied to the determination of lead in water samples with satisfactory results.

1. Introduction

Carbon nanotubes (CNTs), which were discovered in 1991 [1], have been attractive for many research groups for different scientific purposes. Multi-walled carbon nanotubes (MWCNTs) comprise an array of such nanotubes that are concentrically nested. Numerous studies concerning CNTs have been conducted over the past two decades. CNTs have found uses in polymer nanocomposites [2], nanoporouspolymers [3], biomaterials [4], nanofibers [5,6], drug delivery systems [7,8], and analytical applications [9,10]. Because of their uniform structure, CNTs have also been used for the adsorption and removal of various organic and inorganic species [11–13]. Adsorption capacities of CNT have been attenuated by installing various functionalities on the CNT surface [12–14]. These situations are well documented in some reviews [14–16].

Conducting polymer-carbon nanotube composite materials are used in a lot of applications for different specifications of polymers having different functional groups or conjugated π electrons [17–20]. Most notably, conducting polymer-carbon nanotube composites are useful for solid phase extraction of heavy metal ions at trace levels [9,21]. When porous MWCNTs are coated with polypyrrole (PPy), they can gain a higher affinity for metal ions. This may be due to the coordinating ability of the *N* atoms and π electrons on the pyrrole repeating units. The adsorption of lead(II) on new nanocomposite is related to sharing an electron pair of *N* of conducting polymer with lead(II) [21].

In this study, a polymer nanocomposite material has been synthesized and characterized by using multiwalled carbon nanotubes with polypyrrole (MWCNT-PPy). This new conducting polymer nanocomposite has been utilized for the separation and preconcentration of lead(II) at trace levels in water samples, prior to flame atomic absorption spectrometric detection of lead.

2. Experimental

2.1. Instruments

The instrumental detection system used was a Perkin-Elmer Model 3110 flame atomic absorption spectrometer (Norwalk, CT, USA). The equipment was used at conditions recommended by the manufacturer. Air–acetylene burner was used for the determination of the lead(II). A mini homemade micro injection system coupled to the nebulizer with capillary tubing was used for measurement of concentration of lead. For this purpose, 50 μL of the samples were introduced to nebulizer of the AAS with an Eppendorf pipette by using the micro injection system.

The FT-IR spectra of the nanotubes and composite nanotubes were recorded on a Perkin-Elmer Spectrum 400 FT-IR spectrometer (Waltham, MA, USA). Scanning electron microscope (SEM) images were obtained on a LEO 440 SEM. Thermal behavior of the

* Corresponding author. Tel./fax: +90 35 2437 4929.
E-mail address: soylak@erciyes.edu.tr (M. Soylak).

0039-9140/$ - see front matter © 2013 Elsevier B.V. All rights reserved.
http://dx.doi.org/10.1016/j.talanta.2013.11.044

samples was obtained by using a DTA/TG system. The DTA/TG measurements were performed in an alumina crucible, using a Perkin Elmer-Diamond analyzer (heating-cooling rate 10 °C min^{-1}). pH measurements were carried out a Sartorius PT-10 a Metrohm pH meter (Germany) equipped with a combined glass electrode.

2.2. Reagents and solutions

All chemicals were of the highest purity available from Merck and were used as received. Distilled/deionized water (Millipore Milli-Q system) was used for solution preparation. High purity reagents from Sigma-Aldrich (St. Louis, USA) and Merck (Darmstadt, Germany) were used. Standard stock solutions containing 1000 mg L^{-1} of lead(II) were prepared from lead(II) nitrate (Aldrich, Milwaukee, WI, USA) in 1% of HNO_3 into 1 L calibrated flasks. Dilute standard solutions and model solutions were prepared daily from the stock standard solutions.

Pyrrole, HCl, and ammonium persulfate were purchased from Merck Company. Pyrrole was distilled before use. Multiwalled carbon nanotubes (no.: 677248-5G, external diameter: 10–15 nm, internal diameter: 2–6 nm, length: 0.1–10 μm, surface area: 248 m^2 g^{-1}) were purchased from Aldrich, Milwaukee, WI, USA.

Buffer solutions given in the literature [22–24] were used in the present work. SPS-WW2 Waste water Level 2 Certified reference material (CRM) was used from Spectrapure Standards AS, Oslo, Norway.

Thermal water from Sivas, two different waste water samples from plants located in Kayseri Organized Industrial Area and well water from Ankara were collected. Samples used were collected in pre-washed polyethylene containers and were filtered through a Millipore cellulose membrane filter (0.45 μm of pore size).

2.3. Preparation of MWCNT-PPy nanocomposite

The MWCNT-PPy nanocomposite was synthesized according to literature method [9]. First, 40 mL of HCl solution (1 M) containing MWCNTs (0.25 g) was sonicated at room temperature for 15 min. 250 μL of pyrrole was added into the reaction mixture and stirred for half an hour. The solution was then cooled to 0 °C, and a stoichiometric amount of ammonium persulfate, in 1 M HCl solution, was added drop wise to the reaction mixture over a period of 5 h while stirring vigorously. The product was then filtered, washed with methanol/water solution, and finally dried under low pressure for 24 h. A black powder product was obtained. The schematic structure of the nanocomposite was illustrated in Fig. 1.

2.4. Preconcentration procedure

A model solution of 50 mL including 20 μg of lead(II) and 4 mL of phosphate buffer (pH 6) was passed through the column containing 0.20 g of the nanocomposite at a flow rate of 1.5 mL min^{-1}. After the extraction, the retained lead(II) was then eluted from the solid phase with 10 mL of 3 M HNO_3 solution at a flow rate of 2.0 mL min^{-1}. The eluent was evaporated to 1.0 mL at 40 °C on a hot plate in hood. The lead in the final solution was determined by flame AAS using micro injection system.

3. Results and discussion

3.1. Characterization of modified MWCNT with PPy nanocomposite

Fig. 2 illustrates the SEM images of synthesized nanocomposites. The differences between pristine MWCNTs and MWCNT-PPy nanocomposites can be seen in Fig. 2; the specific spun structures of MWCNT fibers in Fig. 2a and polypyrrole coated the MWCNT surface in Fig. 2b. While pristine MWCNTs show spun structures, polypyrrole coated MWCNT exhibit cauliflower-like of images. According to SEM analysis of pristine MWCNTs and MWCNT-PPy, the difference between MWCNTs and MWCNT-PPy, that MWCNTs' surface was completely coated with PPy in the in situ polymerization, can be clearly seen.

There are apparent differences seen from the FT-IR spectrums of pristine MWCNTs and its nanocomposite. According to FT-IR spectrum of pristine MWCNTs, there are some distinct absorption peaks seen at 1100, 1472, 1670, and 3446 cm^{-1} in Fig. 3a. The FT-IR spectrum of MWCNT-PPy in Fig. 3b shows a peak close to 800 cm^{-1} due to the N–H out of plane bending absorption. The band observed near to 900 cm^{-1} is due to the C–H out of plane bending. The C=C stretching of aromatic compounds generally occur in the range of 1000–1100 cm^{-1}. N3H bending of secondary amines is seen at 1385 cm^{-1} and 1540 cm^{-1}. The CåN stretching is observed at 1640 cm^{-1}. Amine (N3H) group N3H stretching can be seen at the region of 3300–3500 cm^{-1}.

According to TGA results of MWCNTs, PPy, and MWCNT-PPy given in Fig. 4; 10% and 50% of weight losses of the pristine MWCNTs are observed at 325 °C, and 1050 °C; however they are seen for MWCNT-PPy at 230 °C, and 1050 °C, and observed for the pristine PPys at 220 °C, and 1050 °C, respectively. Fast degradations of MWCNTs start around at 825 °C. On the other hand, PPy has very fast degradation between 230 °C and 400 °C. When we look at the curves, it can be clearly seen that there are two degradation pathways for MWCNT-PPy, and weight losses of them for any temperature above 230 °C are much more than the pristine MWCNTs. While first degradation starts around 230 °C, the other starts around 800 °C for MWCNT-PPy. All of these results show that our composite material contains a small part of PPy in it.

3.2. Effect of pH

For solid phase extraction of heavy metal ions, the pH of the working media which affect the quantitative recoveries of metal

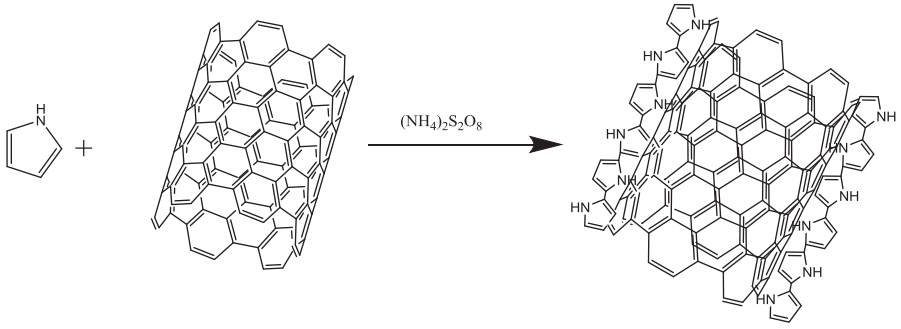

Fig. 1. Schematic structure of the nanocomposite.

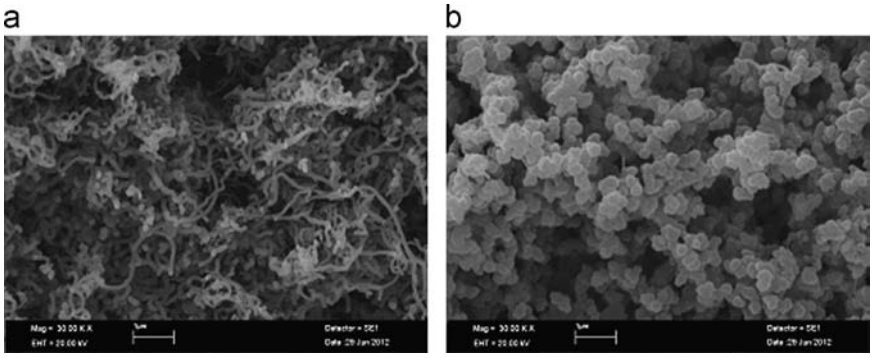

Fig. 2. SEM micrograph images. (a) Pristine MWCNT and (b) MWCNT-PPy nanocomposite.

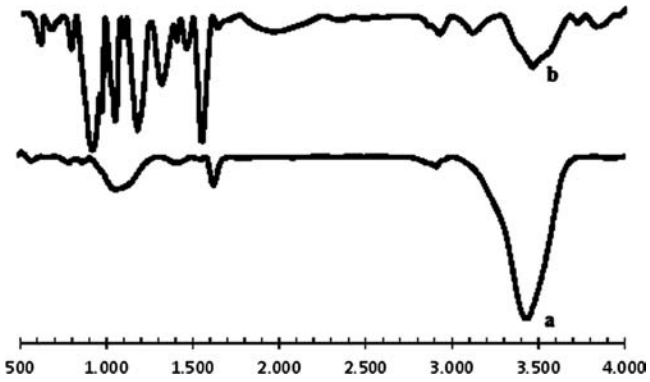

Fig. 3. FT-IR spectrums (a) pristine MWCNTs (b) FT-IR spectrum of MWCNT-PPy.

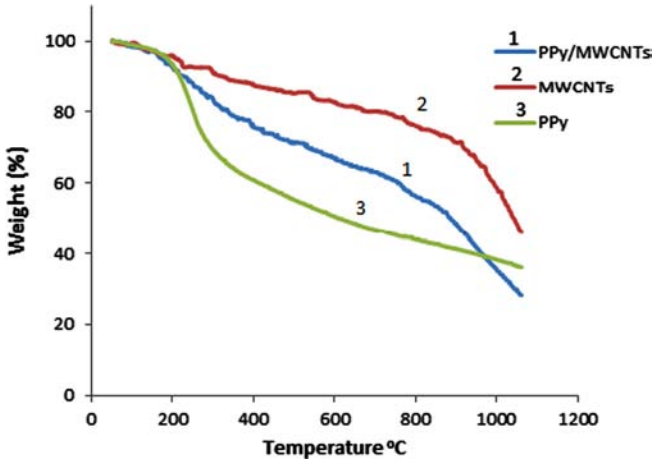

Fig. 4. TGA spectrums (1) MWCNT-PPy (2) MWCNTs (3) PPy.

ions is an important and critical analytical factor [25–28]. Hence, careful attention should be paid to the selection of the suitable working pH. The effect of pH on the recovery of lead was checked in the range of 3.0–8.0 by using buffer solutions of phosphate and acetate. Fig. 5 shows the effect of pH on the recovery of lead(II). Interaction between electron pair of N of conducting polymer on nanocomposite and lead(II) were affective at acidic pHs. The quantitative recovery was obtained between pH 5.5 and pH 6.5. The pH 6.0 was selected for subsequent experiments.

3.3. Selection of eluent type and volume

Various elution solutions were examined (Table 1) and the results show that 3 M HNO_3 is the most suitable eluent. Therefore, 3 M HNO_3 was chosen as the eluent with an eluent flow rate of 2.0 mL min^{-1}. At the same time, the effect of the eluent volume

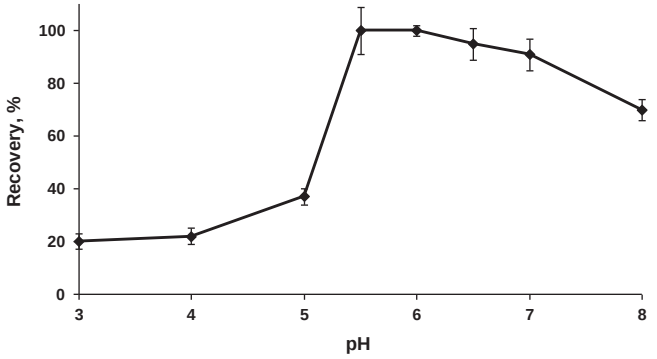

Fig. 5. Effect of pH on the recovery of lead(II) (Conditions: 0.4 μg mL^{-1} of lead(II), model solution volume; 50 mL, eluent: 10 mL of 3 mol L^{-1} nitric acid, amount of nanocomposite: 0.2 g, *N*: 3).

Table 1
Effect of eluent type on the recovery of lead(II) (pH: 6.0, concentration of lead(II): 0.4 μg mL^{-1} of lead(II), model solution volume: 50 mL, eluent flow rate: 2.0 mL min^{-1}, amount of nanocomposite: 0.2 g, *N*: 3).

Eluent solution	Eluent volume (mL)	Recovery (%)
1.0 M HNO_3	10	93 ± 8
2.0 M HNO_3	10	79 ± 6
3.0 M HNO_3	10	100 ± 2
1.0 M HCl	10	88 ± 3
2.0 M HCl	10	82 ± 5
3.0 M HCl	10	61 ± 4
1.0 M CH_3COOH	10	< 5
2.0 M CH_3COOH	10	< 5
3.0 M CH_3COOH	10	11 ± 0

was examined by using 5 and 10 mL of eluent volume and quantitative recovery was obtained with 10 mL of 3 M HNO_3.

3.4. Influences of flow rate of sample solution

The effects of flow rate of sample solution on the recoveries of lead(II) on nanocomposite were investigated in the range of 1.0–5.0 mL min^{-1}. The quantitative recoveries for lead(II) were obtained at the all working range of sample flow rate. 1.5 mL $min^{-1}$was selected as sample flow rate for further studies.

3.5. Effect of sample volume

Sample volume is an important parameter to get high pre-concentration factor and low detection limit [29–36], the influence of sample volume on the recovery of lead was evaluated by passing 25–300 mL of model solutions with a sample flow rate of 1.5 mL min^{-1}. The recoveries of lead(II) were quantitative up to

Table 2
Tolerable levels of interfering ions on recovery of lead(II) (pH: 6.0, concentration of lead(II): 0.4 μg mL^{-1} of lead(II), model solution volume 50 mL, eluent: 10 mL of 3 mol L^{-1} nitric acid, amount of nanocomposite: 0.2 g, *N*: 3).

Ion	Tolerable concentration (μg mL^{11})
K^+, Cl^-	10,000
Na^+	5000
Mg^{2+}, Ca^{2+}, SO_4^{2-}	2500
Ni^{2+}, Cd^{2+}, Cu^{2+}, Co^{2+}	10

Table 3
Recovery studies for the thermal water sample from Sivas and a mine waste water from Yozgat (pH: 6.0, eluent: 10 mL of 3 mol L^{-1} nitric acid, amount of nanocomposite: 0.2 g, *N*: 3).

Added (μg)	Thermal water from Sivas[a]		Mine waste water from Yozgat	
	Found (μg)	Recovery (%)	Found (μg)	Recovery (%)
0	BDL[b]	–	BDL	–
2.0	2.02 ± 0.02[c]	101	2.00 ± 0.14	100
4.0	4.01 ± 0.10	100	3.95 ± 0.10	99
10	10.13 ± 0.58	101	10.14 ± 0.57	101
25	25.80 ± 0.52	103	25.15 ± 1.71	101
30	30.30 ± 1.04	102	29.66 ± 2.76	99

[a] Properties of thermal water sample at the sampling: temperature: 45 °C, pH: 6.81, conductivity: 2750–3380 μs/cm.
[b] BDL: below of detection limit.
[c] Mean ± standard deviation.

200 mL and the recovery was not quantitative for higher volume than 200 mL. The preconcentration factor (PF) was calculated as 200 by the ratio of the highest sample volume (200 mL) and the last volume (1 mL).

3.6. Matrix effects

Matrix effects are one of the critical problem in the flame atomic absorption spectrometric detection of metal ions [37–45], therefore, the effects of some matrix ions on separation and preconcentration of lead(II) by using present work were examined. For this purpose, 50 mL of model solutions containing 20 μg of lead(II) and various amounts of coexisting ions were treated by using developed procedure. The maximum tolerance values of the examined ions are shown in Table 2. It can be seen that most ions in water samples has no obvious effect for determination of lead (II) even at high concentrations.

3.7. Analytical characteristics of the method

The calibration graph using the presented separation–preconcentration system for lead was linear in the range of 2.5–175 μg L^{-1} described by the following equation, $y = 5.39 \times 10^{-3}$ [Pb(II)] + 8.62×10^{-6} (slope: 5.39×10^{-3} and interception: 5.39×10^{-3}) with a correlation coefficient of 0.999, where y is the absorbance signal and concentration of Pb(II) is expressed as μg L^{-1}.

Limit of detection was 1.1 μg L^{-1} (three times of the standard deviation of 11 runs measurements of blank solution). Limit of quantification was 3.7 μg L^{-1} (ten times of the standard deviation of 11 runs measurements of blank solution). The relative standard deviation (RSD) was 5.9% for eleven replicate measurements of 0.4 μg mL^{-1} lead(II).MWCNT-PPy could be reuse as over than 150 times without any loss in its sorption behavior.

Table 4
Analysis of lead(II) in water samples (pH: 6.0, concentration of lead(II): 0.4 μg m L^{-1} of lead(II), volume of water samples: 200 mL, final volume: 1 mL, amount of nanocomposite: 0.2 g, *N*: 3).

Samples	Concentration (μg mL^{-1})
Waste water I	2.16 ± 0.12[a]
Waste water II	0.10 ± 0.01
Well water	0.018 ± 0.0004

[a] Mean ± standard deviation.

3.8. Adsorption capacity and isotherm

Under the optimized SPE conditions, The adsorption isotherm and the adsorption capacity of nanocomposite for lead(II) was studied by the column method. The adsorption capacity (nm) of nanocomposite was obtained by using the Langmuir equation [46] based on the following equation:

$$C/n = (1/n_m\ K) + (1/n_m)\ C$$

C (ng mL^{-1}) is the concentration of lead(II) in model solution and *n* (mg g^{-1}) is the amount of adsorbed lead(II) per gram of nanocomposite at equilibrium. The lead(II) ion concentration in model solution was changed from 8 to 200 μg mL^{-1} for the investigation of adsorption capacity of nanocomposite. The model solution was passed through the column containing 0.2 g nanocomposite. After passing the solution through column, the sample was determined by FAAS. The uptake of lead(II) increases markedly until reaching maximum value at 100 μg mL^{-1} of the sample solutions for lead(II). The adsorption capacity of nanocomposite for lead(III) was found to be 25.0 mg g^{-1}.

3.9. Applications

The addition/recovery tests for the thermal water sample from Sivas and mine waste water from Yozgat were used to prove the accuracy of the developed SPE method. The different amounts of lead(II) were added to the water samples. The results were given in Table 3. A good agreement was obtained between the added and measured lead amounts for both thermal and waste water samples.

The validation of the presented method was checked by the analyzing SPS-WW2 Waste water Level 2 certified reference materials. While the certified value of SPS-WW2 Waste water Level 2 certified reference material was 0.500 ± 0.003 μg mL^{-1}, the lead level was found 0.503 ± 0.003 μg mL^{-1} ($N = 3$). It was found that there was no significant difference between the result obtained and the certified result. The obtained recovery values for accuracy of the method were greater than 95%. It shows that the presented procedure could be used for the determination of lead in water samples.

The suggested method was also used for the determination of lead content in three water samples (two waste water from Kayseri Organized Industrial Area and well water from Ankara) and the results are given in Table 4.

3.10. Comparison of the nanocomposite with literature for solid phase extraction of lead(II)

The comparison results with some other preconcentration methods used for the solid phase extraction of lead(II) are given in Table 5. The proposed method has generally low LOD and good enrichment factor with some exceptions and is comparable with the most of published reports [53–59]. The nanocomposite has a superior reusability and stability. It can be used for all throughout of the present work at least 150 times.

Table 5
Comparisons between the analytical performances of the PPy/MWCNT nanocomposite with different nano absorbents used in solid phase extraction.

Adsorbent	Instrument	Adsorption capacity (mg g^{-1})	LOD (μg L^{-1})	PF	References
Multi-wall carbon nanotubes	FAAS	10.3	0.60	80	[47]
Nano-sized manganese dioxide functionalized multi-wall carbon nanotubes	ETAAS	6.7	0.0044	100	[48]
Multi-wall carbon nanotubes	FAAS	–	8.0	20	[49]
Diethyldithiocarbamate-modified TiO_2 nanoparticles	ICP-AES	19	1.7	33	[50]
Multiwalled carbon nanotubes impregnated with 4-(2-thiazolylazo)resorcinol	FAAS	1	7.2	15	[51]
Modified nano-alumina	FAAS	16.4	0.17	250	[52]
Gold nanoparticle loaded in activated carbon	FAAS	31.6	2.8	200	[53]
Bismuthiol-II-immobilized magnetic nanoparticles	ICP-AES	9.4	0.085	87	[54]
MWCNT-PPy nanocomposite	FAAS	25	1.1	200	This work

FAAS: Flame atomic absorption spectrometry, ETAAS: Electrothermal atomic absorption spectrometry, ICP-AES: Inductively coupled plasma atomic emission spectrometry, PF: preconcentration factor, LOD: Limit of detection.

4. Conclusions

A new MWCNT-PPy nanocomposite has been synthesized and characterized for the solid phase extraction of lead in water samples. The new nanocomposite could be used all throughout of the work without any loss and has high adsorption capacity (25.0 mg lead(II) per gram nanocomposite). The influences of matrix ions of natural water samples are at tolerable levels.

Acknowledgment

The authors are grateful for the financial support of the Units of the Scientific Research Project of Erciyes University and Nigde University.

References

[1] S. Iijima, Nature 354 (1991) 56–58.
[2] Z. Spitalsky, D. Tasis, K. Papagelis, C. Galiotis, Prog. Polym. Sci. 35 (2010) 357–401.
[3] H.S. Kim, H.I. Kwon, Y.S. Yun, H. Bak, J.S. Yoon, J. Nanosci. Nanotechnol. 11 (2011) 4434–4438.
[4] N. Saito, Y. Usui, K. Aoki, N. Narita, M. Shimizu, K. Hara, N. Ogiwara, K. Nakamura, N. Ishigaki, H. Kato, S. Taruta, M. Endo, Chem. Soc. Rev. 38 (2009) 1897–1903.
[5] N. Samadi, V. Shahinfard, J. Biomed. Pharm. Res. 2 (2013) 35–41.
[6] S. Shao, S. Zhou, L. Li, J. Li, C. Luo, X. Li, J. Weng, Biomaterials 32 (2011) 2821–2833.
[7] L. Zhuang, S. Tabakman, K. Welsher, H. Dai, Nano Res. 2 (2009) 85–120.
[8] A.M.A. Elhissi, A. Waqar, I.U. Hassan, V.R. Dhanak, A.J. D'Emanuele, Drug Deliv. (2012) 10, http://dx.doi.org/10.1155/2012/837327. (Article ID 837327).
[9] M.R. Nabid, R. Sedghi, R. Hajimirza, H.A. Oskooie, M. Heravi, Microchim. Acta 175 (2011) 315–322.
[10] H. Zhang, H. Guo, X. Deng, P. Gu, Z. Chen, Z. Jiao, Nanotechnology 21 (2010) 7, http://dx.doi.org/10.1088/0957-4484/21/8/085706. (085706).
[11] A. Duran, M. Tuzen, M. Soylak, J. Hazard. Mater. 169 (2009) 466–471.
[12] F. Zheng, D.L. Baldwin, L.S. Fifield, N.C. Anheier, C.L. Aardahl, J.W. Grate, Anal. Chem. 78 (2006) 2442–2446.
[13] M. Tuzen, M. Soylak, J. Hazard. Mater. 147 (2007) 219–225.
[14] R. Sitko, B. Zawisza, E. Malicka, Trends Anal. Chem. 37 (2012) 22–31.
[15] X. Ren, C. Chen, M. Nagatsu, X. Wang, Chem. Eng. J. 170 (2011) 395–410.
[16] C.H. Latorre, J.Á. Méndez, J.B. García, S.G. Martín, R.M.P. Crecente, Anal. Chim. Acta 749 (2012) 16–35.
[17] M. Baibarac, P. Gómez-Romero, J. Nanosci. Nanotechnol. 6 (2006) 1–14.
[18] N. Samadi, V.J. Shahinfard, Biomed. Pharm. Res. 2 (2013) 35–41.
[19] R. Di Giacomo, B. Maresca, A. Porta, P. Sabatino, G. Carapella, H.C. Neitzert, IEEE Trans. Nanotechnol. 12 (12) (2013) 111–114.
[20] J.C.C. Yu, E.P.C. Lai, React. Funct. Polym. 66 (66) (2006) 702–711.
[21] M.R. Nabid, R. Sedghi, A. Bagheri, M. Behbahani, M. Taghizadeh, H. Oskooie, M.M. Heravi, J. Hazard. Mater. 203 (2012) 93–100.
[22] M. Tuzen, M. Soylak, L. Elci, Anal. Chim. Acta 548 (2005) 101–108.
[23] I. Narin, M. Soylak, K. Kayakirilmaz, L. Elci, M. Dogan, Anal. Lett. 36 (2003) 641–658.
[24] E. Melek, M. Tuzen, M. Soylak, Anal. Chim. Acta 578 (2006) 213–219.
[25] I. Narin, M. Soylak, Anal. Chim. Acta 493 (2003) 205–212.
[26] H.Z. Li, J. Zhang, W.X. Xie, F.Q. Cao, Metall. Anal. 30 (2010) 66–69.
[27] M. Soylak, M. Tuzen, J. Hazard. Mater. 152 (2008) 656–661.
[28] A. Culetu, A.C. Ion, I. Ion, C. Luca, Univ. Politech. Bucur. Sci. Bull. B 72 (2010) 139–146.
[29] U. Divrikli, M. Soylak, L. Elci, Trace Elem. Electrolytes 19 (2002) 177–181.
[30] T. Ikeda, T. Shimizu, N. Uehara, Tetsu to Hagane A 95 (2009) 59–64A.
[31] F.A. Aydin, M. Soylak, Talanta 73 (2007) 134–141.
[32] M. Tuzen, K.O. Saygi, M. Soylak, J. Hazard. Mater. 156 (2008) 591–595.
[33] M. Soylak, L. Elci, J. Trace Microprobe Tech. 18 (2000) 397–403.
[34] R.S.D. Castro, L. Caetano, G. Ferreira, P.M. Padilha, M.J. Saeki, L.F. Zara, M.A. Martines, G.R. Castro, Ind. Eng. Chem. Res. 50 (2011) 3446–3451.
[35] M. Soylak, U. Sahin, L. Elci, Anal. Chim. Acta 322 (1996) 111–115.
[36] Q. Wei, B. Du, D. Wu, Q. Ou, Spectrosc. Spect. Anal. 24 (2004) 1400–1403.
[37] M. Soylak, M. Tuzen, J. Hazard. Mater. 152 (2008) 656–661.
[38] B. Bati, H. Cesur, Anal. Sci. 18 (2002) 1273–1274.
[39] S. Saracoglu, M. Soylak, L. Elci, Chem. Anal. Warsaw 48 (2003) 77–85.
[40] S. Kartikeyan, B. Vijayalekshmy, S. Chandramouleeswaran, T.P. Rao, C.S.P. Iyer, Anal. Lett. 30 (1997) 1037–1050.
[41] M. Soylak, L. Elci, M. Dogan, J. Trace Microprobe Tech. 19 (2001) 329–344.
[42] A. Uzun, M. Soylak, L. Elci, M. Dogan, Asian J. Chem. 14 (2002) 1277–1281.
[43] M. Tuzen, D. Citak, D. Mendil, M. Soylak, Talanta 78 (2009) 52–56.
[44] M. Soylak, I. Narin, L. Elci, M. Dogan, Trace Elem. Electrolytes 16 (1999) 131–134.
[45] M. Soylak, A.U. Karatepe, L. Elci, M. Dogan, Turk. J. Chem. 27 (2003) 235–242.
[46] I. Langmuir, J. Am. Chem. Soc. 40 (1918) 1361–1403.
[47] M. Tuzen, K.O. Saygi, M. Soylak, J. Hazard. Mater. 152 (2008) 632–639.
[48] B. Yang, Q. Gong, L. Zhao, H. Sun, N. Ren, J. Qin, J. Xu, H. Yang, Desalination 278 (2011) 65–69.
[49] S.G. Ozcan, N. Satiroglu, M. Soylak, Food. Chem. Toxic. 48 (2010) 2401–2406.
[50] H. Zheng, X. Chang, N. Lian, W. Sui, Y. Cui, Int. J. Environ. Anal. Chem. 86 (2006) 431–441.
[51] Z.A. ALOthman, M. Habila, E. Yilmaz, M. Soylak, Microchim. Acta 177 (2012) 397–403.
[52] M. Ezoddin, F. Shemirani, K. Abdib, M.K. Saghezchi, M.R.J. Jamali, J. Hazard. Mater. 178 (2010) 900–905.
[53] G. Karimipour, M. Ghaedi, M. Sahraei, R. Daneshfar, M.N. Biyareh, Biol. Trace Elem. Res. 145 (2012) 109–117.
[54] J.S. Suleiman, B. Hu, H. Peng, C. Huang, Talanta 77 (2009) 1579–1583.
[55] M. Soylak, I. Murat, Food Anal. Methods 5 (2012) 1003–1009.
[56] H.T. Ham, C.M. Koo, S.O. Kim, Y.S. Choi, I.J. Chung, Macromol. Res. 12 (2004) 384–390.
[57] S. Wang, Y. Li, G. Xiaoyan, H. Zhao, Z. Luan, C. Xu, D. Wu, Chin. Sci. Bull. 48 (2003) 441–443.
[58] M. Soylak, F. Armagan, L. Elci, M. Dogan, Ann. Chim. (Rome) 91 (2001) 637–647.
[59] B. Mandal, U.S. Roy, Indian J. Chem. A 47 (2008) 1497–1502.